

A Unifying Framework to Quantify the Effects of Substrate Interactions, Stiffness, and Roughness on the Dynamics of Thin Supported Polymer Films

Paul Z. Hanakata*,¹ Beatriz A. Pazmiño Betancourt,^{1,2} Jack F. Douglas^{†,2} and Francis W. Starr¹

¹*Department of Physics, Wesleyan University, Middletown, CT 06459, USA*

²*Materials Science and Engineering, National Institute of Standards and Technology, Gaithersburg, Maryland 20899, USA[‡]*

(Dated: March 4, 2022)

Changes in the dynamics of supported polymer films in comparison to bulk materials involve a complex convolution of effects, such as substrate interactions, roughness and compliance, in addition to film thickness. We consider molecular dynamics simulations of substrate-supported, coarse-grained polymer films where these parameters are tuned separately to determine how each of these variables influence the molecular dynamics of thin polymer films. We find that all these variables significantly influence the film dynamics, leading to a seemingly intractable degree of complexity in describing these changes. However, by considering how these constraining variables influence string-like collective motion within the film, we show that all our observations can be understood in a unified and quantitative way. More specifically, the string model for glass-forming liquids implies that the changes in the structural relaxation of these films are governed by the changes in the average length of string-like cooperative motions and this model is confirmed under all conditions considered in our simulations. Ultimately, these changes are parameterized in terms of just the activation enthalpy and entropy for molecular organization, which have predictable dependences on substrate properties and film thickness, offering a promising approach for the rational design of film properties.

I. INTRODUCTION

Polymer films are used in a wide variety of applications, ranging from micro-electronic devices to artificial tissues [1, 2]. However, both mechanical and dynamical properties of polymeric materials often change considerably in relation to bulk once confinement dimensions become less than $\simeq 100$ nm. Much of the effort aimed at understanding the property changes in thin polymer films has centered on measurements related to the stiffness of these films [3, 4] and changes of molecular mobility, as quantified by the glass-transition temperature T_g [5, 6]. Many experimental [5, 7–14], as well as computational [15–20] studies, have reported large property changes in thin films. These changes have been mainly attributed to a combination of substrate interaction and geometrical confinement. There is also a growing awareness of the relevance of substrate roughness and stiffness, as well as non-equilibrium residual stress effects in cast films. It is a difficult matter to separate all of these different effects in experiments, and the present work addresses this general problem through molecular dynamics simulations of substrate-supported, coarse-grained polymer melt films of variable thickness where the polymer-substrate interaction is varied, along with the boundary roughness and rigidity. Since we can tune these parameters in simulations, we can obtain clear indications of

how each of these variables influence the film molecular dynamics. After an analysis of how these diverse factors affect basic dynamic properties of the polymer film, we show that the dynamical changes under all these conditions can be organized and understood in terms of how these constraining variables influence collective motion within the film, parameterized by the enthalpy and entropy of activation for molecular reorganization.

Changes in T_g in polymer films are usually associated with local changes in the dynamics near the interfaces. Many studies have reported that a repulsive or neutral substrate along with a free boundary leads to an enhancement in dynamics and a reduction of T_g [8, 19, 21, 22]. In contrast, an attractive substrate, which typically slows down the dynamics near the substrate, results in an increase in T_g [5, 8, 10–13, 15, 17, 20, 23–25]. However, an attractive smooth substrate with a relatively weak interaction may also enhance the rate of relaxation and diffusion [9, 11, 13, 15, 26, 27], demonstrating that the polymer-substrate strength and the substrate roughness can also have significant effects on the polymer film dynamics. In particular, it has been noted that the enhancement or slowing of relaxation in supported films induced by two interfaces with different properties can complicate the interpretation of the thickness dependence of T_g [8, 11, 19–21, 23–25, 27].

The most prevalent type of polymer films are those supported on solid substrates, where the relaxation time is often increased near the substrate, while decreased at the free boundary. Additionally, experiments on multi-layered interfacial films have shown that the effects of the free boundary region can be largely eliminated by placing films between stacks of nano-layered polymers with different species [28], suggesting that there is a length scale associated with the interfacial film dynamics. This leads to

*current address: Department of Physics, Boston University, Boston, MA 02115

[†]Official contribution of the U.S. National Institute of Standards and Technology - Not subject to copyright in the United States

[‡]Electronic address: bpazminobeta@wesleyan.edu

the question of whether the film dynamics depends simply on the substrate interaction, or are there other physically relevant characteristics of the interface that must be considered. After all, glass formation is a dynamical phenomenon, so that other variables – such as substrate rigidity – might be relevant. This motivates an exploration of the effects of substrate rigidity on properties of thin polymer films, a property that can be greatly tuned in polymeric materials through cross-linking or through control of the molecular structure [29–31]

A popular picture to rationalize the changes of the film dynamics is a superposition of polymer layers with locally varying dynamics. In this simple model, any changes in the overall dynamics should be manifested locally. Thus, the interfacial layers are correspondingly expected to be the primary contributor to changes in the overall film dynamics. Near an attractive substrate, the polymers are ‘bound’ to the surface, leading to slower dynamics, while at the free boundary region of a supported or free-standing film, the chains have a relatively higher mobility. At the film center, far from both interfaces, the local properties are expected to be ‘bulk-like’. This layer picture of film dynamics is often conceptually linked to local changes in density profile or free volume. In our previous work, we found inconsistencies for this free-volume layer (FVL) rationale for explaining the observed changes in the dynamics [27]. Moreover, the dynamics can be enhanced at the substrate, despite an increase in local density. We also quantified the length scales of both density and dynamical perturbations within supported films and found that the temperature dependence of these scales are opposite to that at the free boundary region, inconsistent with the FVL approach. The changes in the dynamics of the film with a supporting layer are generally *non-local*, so it is naive to treat the film interior as being the same as bulk material.

Here, we consider the dependence of the dynamics on film thickness, substrate roughness, and rigidity. We find that these parameters can induce significant changes in the dynamics, characterized by changes in the film T_g and fragility, but only rather subtle changes are observed in static properties, such as density. Again, we find that free volume ideas are not useful in predicting dynamics at the local level. Rather, substrate interaction, substrate roughness, and stiffness can all greatly influence the mobility gradient transverse to the substrate. Our findings for the variation of T_g with substrate roughness and interaction strength are consistent with earlier works [10, 15, 32, 33], but our observations on fragility and regarding substrate stiffness are new. Another novel aspect of the current work is that we characterize the fragility changes in terms of cooperative motion within the film and, in this way, obtain a *quantitative* understanding of the wide variations in the temperature dependence of the structural relaxation time with film boundary conditions and thickness.

There is continued interest in the breakdown of the Stoke-Einstein relation in glass-forming liquids and the

possible relation of this phenomena with fragility and dynamical heterogeneity, and several recent studies have suggested specific relationships. Since we are able to tune the fragility over a large range using the same polymer model through modifications of confinement, we can assess the validity of these relations in our glass-forming polymer model. We find that the decoupling exponent relating the structural relaxation time to a diffusion relaxation time can be systematically varied with confinement. The degree of decoupling increases as the effective dimension is reduced, i.e., smaller film thickness, consistent with recent observations for model glass-forming liquids in a variable spatial dimension [34]. Moreover, film fragility can either increase or decrease under confinement, depending on the boundary interaction, so we do not generally see an increase in decoupling with greater fragility, as suggested by crystallization measurements in non-polymeric materials [35]. Our results support recent observations [34] that indicate that changes in spatial dimensionality are relevant to understanding the decoupling phenomenon.

Given the sensitivity of the dynamics to the large collection of substrate properties, the question remains: how do we obtain a unified understanding of all these effects on the polymer dynamics? There has been much speculation that these changes revolve around changes in the collective dynamics of the polymer molecules, where the Adam-Gibbs theory is often discussed without a specific definition of the hypothetical ‘cooperatively rearranging regions’ (CRR) that are relevant to understanding these property changes. Simulations have identified cooperative rearrangements that are quantitatively linked to the structural relaxation time for bulk polymer materials [36], and a similar connection has also been established in model polymer nanocomposites [37, 38]. These string-like motions therefore offer a molecular realization of the abstract CRR. We test this predictive scheme for the molecular dynamics simulations of polymer films where the inherent inhomogeneity of the dynamics of these materials makes it unclear whether the model should still apply. Encouragingly, we obtain a remarkable reduction of all our simulation data for structural relaxation in thin polymer films based on this unifying framework. Lastly, we investigate the influence of confinement on the activation free energy parameters that define our description.

II. MODELING AND SIMULATION

We model polymers as unentangled chains of beads linked by harmonic springs. The substrate is modeled either as a collection of substrate atoms, or by a perfectly smooth substrate. Non-bonded monomers or atoms of the substrate interact with each other via the Lennard-Jones (LJ) potential, and we use a shifted-force implementation to ensure continuity of the potential and forces at the cutoff distance r_c . We choose $r_c = 2.5\sigma_{ij}$ to in-

clude inter-particle attractions where σ_{ij} is the monomer “diameter” in the LJ potential. The index pair ij distinguishes interactions between monomer-monomer (mm), substrate-monomer (sm), and substrate-substrate (ss) particles. The LJ interaction is not included for the nearest-neighbors along the chain. These monomers are connected by a harmonic spring potential $U_{\text{bond}} = \frac{k_{\text{chain}}}{2} (r - r_0)^2$ with bond length $r_0 = 0.9$ (equilibrium distance) and spring constant $k_{\text{chain}} = (1111)\epsilon_{\text{mm}}/\sigma_{\text{mm}}^2 \cdot r_0$. The spring constant is chosen as in Ref. [26], but we choose r_0 smaller than in Ref. [26] because we found crystallization occurs readily in the films for the value used in Ref. [26].

The interaction between monomers and the smooth substrate is given by,

$$V_{\text{smooth}} = \frac{2\pi}{3} \epsilon_{\text{sm}} \rho_s \sigma_{\text{ss}}^3 \left[\frac{2}{15} \left(\frac{\sigma_{\text{sm}}}{z} \right)^9 - \left(\frac{\sigma_{\text{sm}}}{z} \right)^3 \right], \quad (1)$$

where z is the distance of a monomer from the substrate. This is the same smooth substrate model that we studied in our previous work [27]. To model the rough substrate, we tether the substrate atoms to the sites of triangular lattice (the 111 face of an FCC lattice) with harmonic potential,

$$U_s(r_i) = \frac{k_s}{2} \left(|\vec{r}_i - \vec{r}_{\text{ieq}}| \right)^2, \quad (2)$$

where \vec{r}_{eq} denotes an equilibrium position on the triangular lattice and k_s is the harmonic spring constant [17]. We choose the lattice spacing to be $2^{1/6} \sigma_{\text{ss}}$, where $\sigma_{\text{ss}} = 0.80 \sigma_{\text{mm}}$ and $\sigma_{\text{sm}} = \sigma_{\text{mm}}$. All values are in reduced units, where $\sigma_{\text{mm}} = 1$ and $\epsilon_{\text{mm}} = 1$. Varying k_s allows us to examine the role of substrate rigidity on the polymer dynamics. We simulate films of variable thicknesses with $N_c = 200, 300, 400, 600$, or 1000 chains of 10 monomers each. These sizes correspond to thicknesses with value of roughly 6 to 25 monomer diameters. We use various interaction strengths ($\epsilon_{\text{sm}} \equiv \epsilon$) between the rough substrate and polymers, ranging from 0.4 to 1.0 ϵ_{mm} with a fixed surface rigidity $k_s = 100$; we vary the strength of the substrate rigidity ($k_s \equiv k$) over the range from 10 to 100 with a fixed $\epsilon = 1$. For this range of model parameters, we find T_g of the film can be higher or lower than the bulk value. Additionally, we simulate a pure bulk system of 400 chains of $M = 10$ monomers each at zero pressure for the purpose of comparison.

We define film thickness $h(T)$ as a distance from the substrate where the density profile along the z direction, perpendicular to the substrate, $\rho(z)$ decreases to 0.10. Other reasonable criteria does not affect our qualitative findings. The resulting $h(T)$ is well described by an Arrhenius form, which we use to extrapolate the thickness value $h_g \equiv h(T_g)$ at the glass transition.

To quantify the overall dynamics of the films and bulk system, we evaluate the coherent intermediate scattering

function,

$$F(q, t) \equiv \frac{1}{NS(q)} \left\langle \sum_{j, k_s=1}^N e^{-iq \cdot [r_k(t) - r_j(0)]} \right\rangle \quad (3)$$

where r_j is the position of monomer j and $S(q)$ is the static structure factor. We define the characteristic time τ by $F(q_0, \tau) = 0.2$, where q_0 is the location of the first peak in of $S(q)$. To quantify dynamics locally within the film, we use the self (or incoherent) $F_{\text{self}}(z, q, t)$ part (*i.e.* $j = k$) of Eq. (3) on the basis of the position z of a monomer at $t = 0$. We define the relaxation time $\tau_s(z)$ by $F_{\text{self}}(z, q_0, \tau_s) = 0.2$.

III. DEPENDENCE OF T_g AND FRAGILITY ON SUBSTRATE STRUCTURE

A. Survey of Substrate Roughness and Film Thickness Effects

We first contrast the overall changes to glass formation of polymer films with various thicknesses supported on a rough or smooth substrate having the same substrate-monomer interaction ($\epsilon = 1.0$). Relative to the bulk system, the relaxation time τ of polymer films on the smooth substrate decreases as we decrease film thickness, and these deviations become more pronounced as we go to lower T , consistent with previous studies [26, 27] (Fig. 1(b)). However, we find the opposite trend for the rough substrate, as noted in Ref. [39, 40]. As we will see, this trend depends on substrate interaction strength and rigidity. We see that the dynamics change more rapidly with T for thinner films resulting in a larger τ relative to the bulk material (Fig. 1(a)). We estimate T_g by fitting our data to the Vogel-Fulcher-Tammann (VFT) equation,

$$\tau(T) = \tau_{\infty} e^{DT_0/(T-T_0)}. \quad (4)$$

where τ_{∞} is an empirical prefactor normally on the order of a molecular vibrational time (10^{-14} to 10^{-13} s) [41], D is a measure of ‘fragility’ and T_0 is a temperature at which τ extrapolates to infinity. Eq. 4 should only be applied above the glass transition temperature. In a lab setting, T_g is often defined as T at which the relaxation time reaches 100 s [42], and we adopt this simple criteria. Figure 1(c) shows that, relative to the bulk, T_g of polymer films on the rough substrate increases with decreasing film thickness, while for the smooth substrate systems, T_g decreases with decreasing film thickness.

The variation in T dependence of relaxation is quantified by fragility, defined as the logarithmic slope of relaxation time at T_g

$$m(T_g) \equiv \left. \frac{\partial \ln \tau}{\partial (T/T_g)} \right|_{T_g}. \quad (5)$$

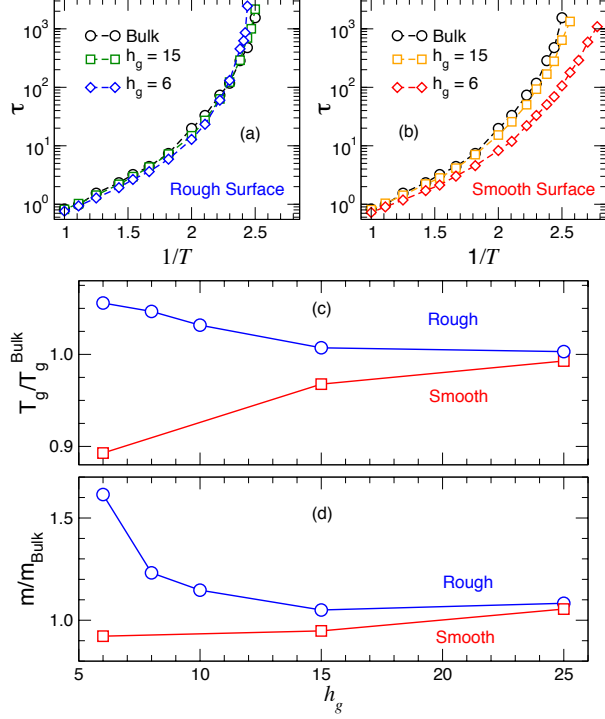


FIG. 1: Effects of film thickness and structure of the supporting substrate on glass transition temperature T_g and fragility. The T dependence of relaxation time τ of a bulk system and two representative film thicknesses h_g supported on (a) a rough or (b) smooth substrate ($\varepsilon = 1$). In this T range, it is apparent that, relative to the bulk, τ increases as the film thickness is decreased on rough substrates, while for smooth substrates shows an opposite behavior. (c) Relative T_g and (d) relative fragility m to the bulk as function of film thickness. Both T_g and m for the rough substrates increase, while T_g and m of smooth substrates decrease as we decrease film thickness.

We evaluate fragility m using the fit of Eq. (4). In Fig. 1(d), we see that, relative to the bulk, films on the rough substrate become more fragile as we decrease thickness, which is apparent from the increasingly rapid variation of $\tau(T)$ (Fig. 1(a)). In contrast, the fragility of polymer films on the smooth substrate decreases weakly with decreasing film thickness.

Experimentally, T_g is often found to be proportional to m [43]. We also find a correlation between T_g and m for both substrates, but this relation is not strictly proportional. Note that films supported on a smooth substrate may have a non-monotonic thickness dependence of T_g and m on thickness. Specifically, our recent work [27] showed that T_g or m decreases with decreasing film thickness on the smooth substrate up to some critical thickness, but that T_g increases for very thin films when interfacial effects become dominant.

B. Local Structure and Dynamics

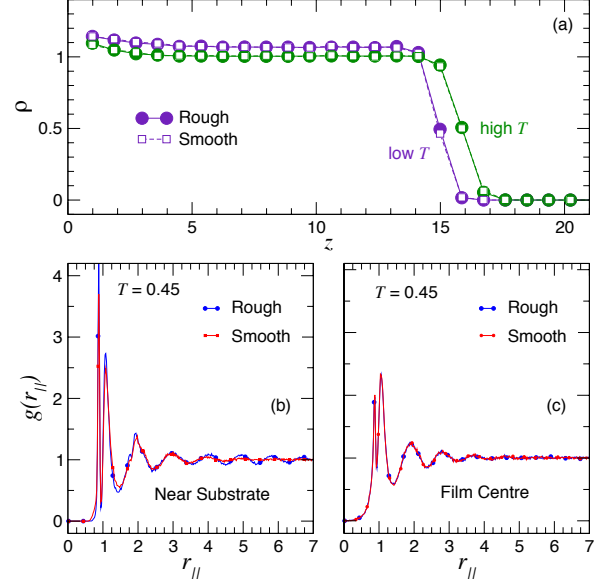


FIG. 2: (a) Monomer density profile $\rho(z)$ of a film, $h_g = 15$, supported on a rough or smooth substrate. (b) Pair-pair correlation function in the direction parallel to the substrate $g(r_{\parallel})$ near the substrate. (c) $g(r_{\parallel})$ at the film center. Monomers near the rough substrate are slightly more densely packed and have better local ordering in comparison to those near the smooth substrate.

To understand the observed changes in T_g and fragility, we resolve both structure and dynamics locally, since the changes in the properties of the film as a whole should be manifested in its local properties. We first contrast the local dynamics and monomer density as function of distance z from the substrate boundary of rough or smooth substrates with monomer-substrate interaction strength $\varepsilon = 1$. We evaluate both $\rho(z)$ and $\tau_s(z)$ with a bin size $\delta z = 0.875$.

In figure 2(a), we observe that the monomer density near either the smooth or rough substrate increases weakly, and has a steady value through most of the film. The density drops to zero over a narrow window at the free boundary region. At the center of the film, the density has a value close to the bulk. The density profile of the film on smooth substrate is essentially identical to that of a film on a rough substrate.

In addition, we contrast the local structure parallel to the substrate by evaluating the density pair correlation function $g(r_{\parallel})$ (see Fig. 2(b) and (c)). Far from the substrate, $g(r_{\parallel})$ of both systems is indistinguishable, as the monomers are completely unperturbed by the substrate. Near the substrate, we see that there is a slight difference in the local structure. In particular, near the substrate, $g(r_{\parallel})$ of the rough substrate has a somewhat larger first peak, indicating that the monomers near the rough sub-

strate are more ordered than those near the smooth substrate. In addition, there is a weak long-range ordering of monomers for the rough substrate, potentially induced by the periodicity of the substrate atoms.

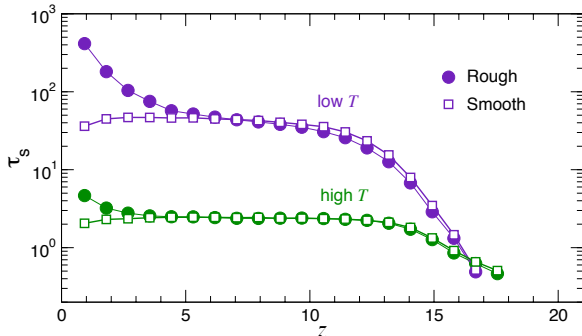


FIG. 3: Relaxation time τ_s as function of distance z from the substrate. Although the averaged densities of two systems are identical, the local dynamics is clearly distinct from one another, particularly near the the substrate.

We next examine to what degree the local film dynamics reflect the changes in the density described above. Figure 3 shows that the dynamics of the film on a rough or smooth substrate at the same T are nearly identical over the range from the center of the film to the free boundary region. However, there are large differences of relaxation time near the substrate. The local relaxation time τ_s increases close to the rough substrate, but decreases near the smooth substrate. The enhanced dynamics near the smooth substrate are in part a consequence of the fact the monomers can “slide” along the substrate due to the substrate smoothness (see Refs. [27, 44]). This effect disappears for a rough substrate. An increasing relaxation time approaching the rough substrate has also been observed in a computational study of a binary Lennard-Jones liquids, as well as in a bead-spring model of polymer melts with a relatively strong interaction, [16, 17, 39, 40]. Evidently, substrate roughness is highly relevant for the polymer film dynamics, and this factor must be controlled for consistent results.

A convenient way to parameterize local dynamical changes is by considering the local dependence of T_g and m as function of distance z from the substrate. This provides a way of summarizing the behavior of $\tau_s(z, T)$, shown in Fig. 3. Figure 4 (a) shows that T_g increases near the rough substrate, reflecting the observed increase of τ_s near the attractive substrate. Near the free boundary region, T_g decreases due to the enhanced mobility of monomers at the free boundary region. For relatively thick films, we find that there is a substantial film region where monomers have a T_g close to the bulk value. This is a situation in which the film thickness is large compared to the perturbing scales of the interfaces [27]. T_g

is often found to be proportional to m , as observed in the overall dynamics. However, we do not see this proportionality between the local T_g and m . Specifically, m decreases approaching the rough substrate while T_g increases. This opposing trend has also been observed in polymer-nanoparticle composites [38].

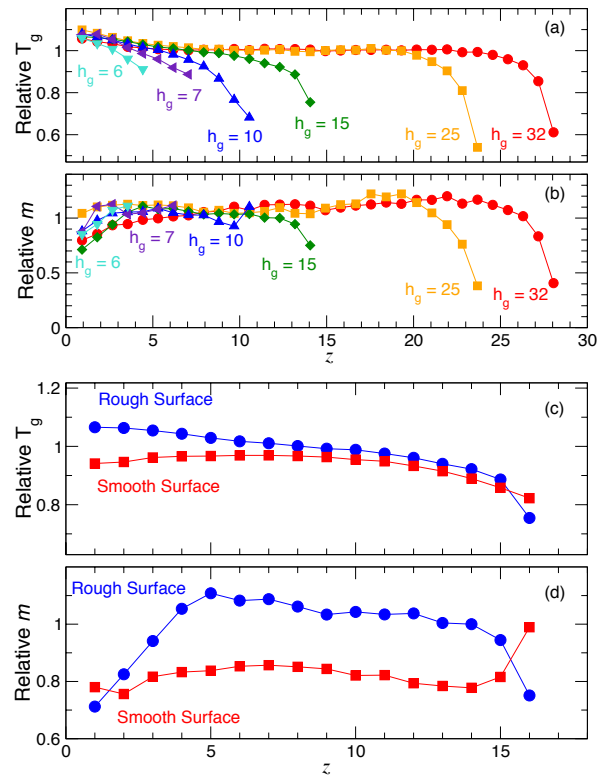


FIG. 4: Local T_g and fragility. (a) Relative T_g and (b) m of polymer films supported on rough substrate as function of distance z from the substrate for many thicknesses. (c) Relative T_g and (d) m of a polymer film ($h_g = 15$) supported on a rough or a smooth substrate. Near the free substrate T_g decreases for both system. Near the substrate, T_g increases for film supported on rough substrate, but decreases for smooth substrate.

Figures 4 (c) and (d) contrast the local variation of T_g and m for rough and smooth substrates of a relatively thick film, $h_g = 15$. In contrast to the increasing T_g of polymer films near the rough substrate, T_g of smooth substrate decreases close to the smooth substrate, which is consistent with variation of τ_s (Fig. 3). Note that T_g and m are slightly depressed for films on the smooth substrate, even at the middle of the film, a scenario where the perturbing scales of both interfaces become comparable to film thickness.

IV. DEPENDENCE OF DYNAMICS ON SUBSTRATE STRENGTH AND RIGIDITY

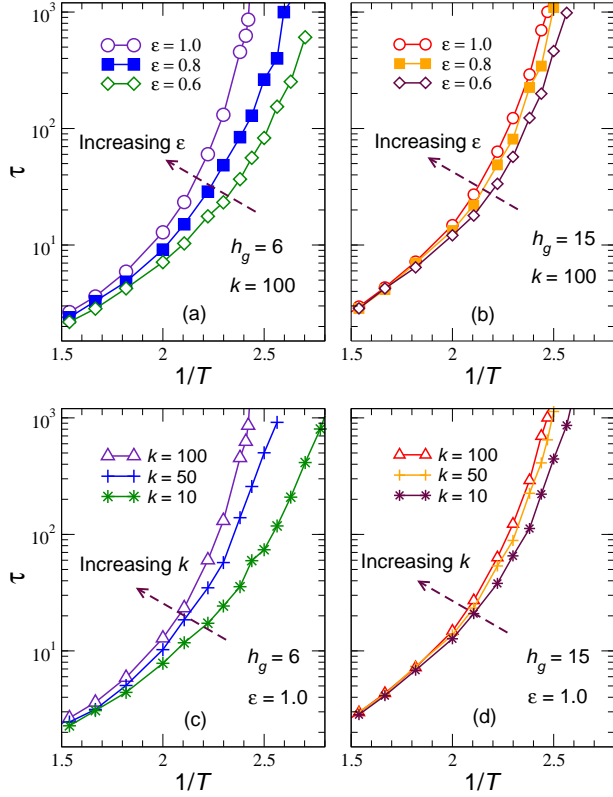


FIG. 5: The T dependence of the relaxation time τ for two film thicknesses, $h_g=15$ and 6, with various interfacial strength ε (a) and (b), and fixed rigidity $k=100$. Panels (c) and (d) show the effect of variable rigidity k for fixed $\varepsilon=1.0$. In general, τ is decreased as we decrease the substrate strength or the molecular-substrate stiffness.

A. Survey of Substrate Interaction and Rigidity Effects

Substrate roughness is relevant to the film dynamics, but there are other crucial variables. We next investigate the dependence of dynamics on the interaction strength as well as rigidity of the rough substrate. First, we examine the role of substrate interaction strength. Figures 5 (a) and 5 (b) show how relaxation time τ for two representative film thicknesses changes as we vary the interaction ε between the rough substrate and the polymers. The overall changes in dynamics result from the competing effects of the substrate and free interface, so that τ can be higher or lower relative to the bulk. As we have established, the free boundary region decreases τ while a substrate with a relatively strong interaction increases τ . Thus, for a given thickness, τ decreases with decreasing the substrate interaction strength.

We find a similar effect by varying the stiffness k of the bonds describing the substrate stiffness. Specifically, increasing the flexibility of the substrate (decreasing k) results in a smaller τ (Fig. 5 (c) and (d)). Evidently, monomers of the chains near the substrate are less constrained, since the substrate atoms are more flexible. The complete local analysis of the dependence of dynamics on flexibility of the substrate will be discussed in the next subsection. By comparing Figs. 5 (a) and (b), as well as (c) and (d), we can see that the substrate interaction or the flexibility of the substrate have greater influences on the thinner film, expected since the thinner film has a larger surface-to-volume ratio.

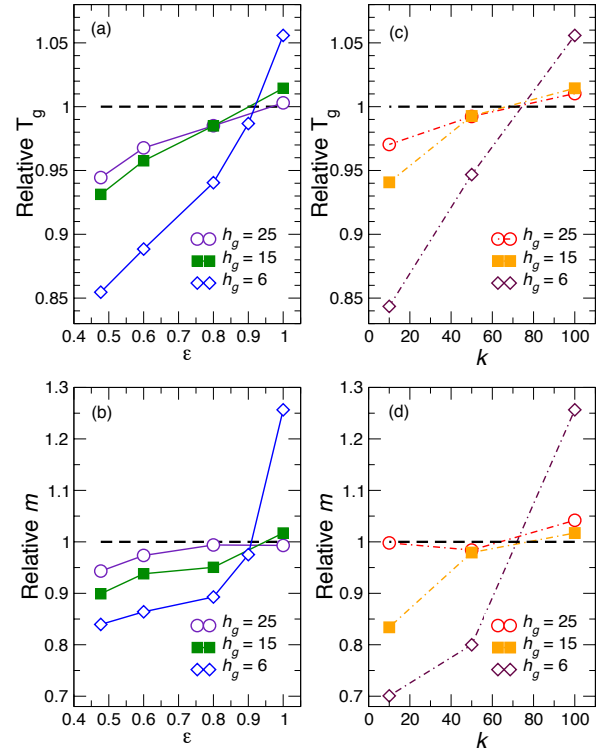


FIG. 6: Dependence of the relative T_g and m of three representative film thicknesses as a function of substrate strength ε (a) and (b) or substrate rigidity k (c) and (d). For thinner films, the range of T_g and m is wide due to the larger substrate-to-volume ratio.

We next evaluate the resulting dependence of T_g and fragility on the substrate interaction strength and rigidity of the rough substrate films. Figures 6 (a) and (b) show how T_g of three representative thicknesses change as a function of substrate interaction strength ε at fixed rigidity $k=100$. Generally, increasing the polymer-substrate interaction increases both T_g and fragility as monomer dynamics near the substrate presumably become progressively slower. These general trends of a de-

creasing T_g with decreasing substrate interaction have also been observed both in experiments and computational works [10, 15, 32, 33]. This depression of fragility is also consistent with the findings in a free-standing film [18], which formally corresponds to taking the limit $\varepsilon \rightarrow 0$. Evidently, the dependence of substrate polymer interaction of T_g or m becomes more significant for thinner films, as indicated by a steeper variation of T_g or m with ε .

We found similar trends for T_g and m by varying the substrate rigidity. That is, increasing substrate rigidity k at fixed substrate interaction strength ($\varepsilon = 1$) increases both T_g and m . It is interesting to note that there appears to be a nearly fixed point for T_g and m as function of ε . Specifically, T_g and m are independent of film thickness for $\varepsilon \simeq 0.9$ ($k = 100$) or $k \simeq 75$ ($\varepsilon = 1$). We emphasize that this does not mean there are no changes in local dynamics, but rather that there is a balance between the dynamic enhancement at the free boundary region and the slowing down of the dynamics near the substrate. In fact, the increasing behavior of m with decreasing thickness is only observed for values $k > 75$ and $\varepsilon > 0.9$. This compensation effect is reminiscent of the self-excluded volume interactions of polymers in solution near their θ point [45, 46], and the compensation point for isolated polymers interacting with surfaces [47].

Both results potentially offer us insights into how T_g changes in multilayer films, which are “stacks” of polymer films with different species characterized by different flexibility, inter-polymer interaction, or molecular weight. Multilayer film experiments by Torkelson and co-workers have shown that a given layer of the multilayer film may have different T_g depending on the properties of neighboring layers [28]. Here, we emphasize that changes in dynamics do not necessarily arise from the substrate interaction strength alone; changes in the rigidity of the interface (e.g. polymer films placed on a polymer substrate with the same substrate interaction strength, but having different molecular flexibility) and substrate roughness are also relevant.

B. Local Structure and Dynamics

We revisit our analysis of both film structure and dynamics (as in the previous subsection) to further confirm our arguments about the role of substrate changes on the overall dynamics. Figures 7 (a) and (c) show how the monomer density $\rho(z)$ changes by varying the substrate strength or rigidity of the substrate. Far from either substrate, $\rho(z)$ has a nearly constant value that is close to the bulk value. In general, the density near the substrate increases slightly, as we increase ε or k . The behavior of the density at very low rigidity ($k = 10$) differs from more rigid substrates. These most flexible substrates can be thought of as an amorphous solid that does not perturb the film much, because it can not adapt its structure to that of the polymer film.

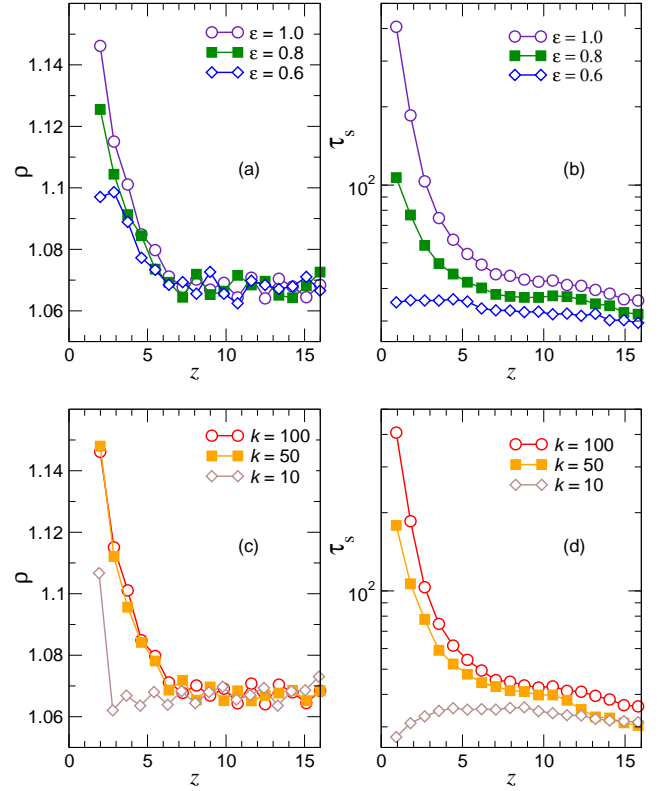


FIG. 7: Variation monomer of the density profile $\rho(z)$ and local relaxation time τ_s as function of distance z from the substrate with varying polymer-substrate interaction ε (a) and (b) or substrate rigidity k (c) and (d). Note that ρ becomes nearly constant for $z > 6$, but for $z < 6$, ρ depends sensitively on the interaction at the boundary.

Similar to our findings comparing rough and smooth substrates, Figures 7(b) and (d) show substantial changes in local relaxation τ_s at the substrate as function of ε or k . Local relaxation time $\tau_s(z)$ generally decreases as we decrease ε or k . The weaker substrate interaction allows monomers to avoid caging near the attractive substrate. Likewise, decreasing substrate rigidity allows monomers to move freely, since the substrate atoms are not strongly localized. These dynamical changes do not mirror the changes in the local density. This again emphasizes the limitations of a free volume based interpretation of results..

V. DECOUPLING AND THE ‘FRACTIONAL’ STOKES-EINSTEIN RELATION

One of the canonical features of glass-forming liquids is that the decoupling of viscous and diffusive relaxation processes gives rise to a breakdown of the Stokes-Einstein (SE) relation approaching the glass transition. This ‘decoupling’ phenomenon is frequently associated with the

emergence of heterogeneity of the dynamics, which we know is prevalent in our thin polymer films. Normally, decoupling is quantified by the relation between the diffusion coefficient D and viscosity or a collective relaxation time. For polymer chains, D is not readily accessible computationally since the mean-square displacements $\langle r^2(t) \rangle$ of the chain center of mass only reaches the diffusive regime after extremely long times when the polymer melt is cooled. Instead, reference [36] has offered evidence that the characteristic time t^* at which the non-Gaussian parameter,

$$\alpha_2(t) = \frac{3\langle r^4(t) \rangle}{5\langle r^2(t) \rangle^2} - 1, \quad (6)$$

has a maximum provides a diffusive relaxation time that exhibits a decoupling relation to the α relaxation time τ of the segmental dynamics.

To broadly characterize the heterogeneity of segmental motion and estimate a diffusive time scale, Fig. 8 shows $\alpha_2(t)$ for many T for $h_g = 15$ with a rough or attractive substrate. Data for other thickness and substrate interactions show the same qualitative features, so we only show this representative example. As is widely appreciated, α_2 exhibits a peak at intermediate time t^* . One unusual feature of these data is that $\alpha_2(t)$ does not decay to zero for large t , reflecting the fact that displacement perpendicular to the substrate is intrinsically limited by film thickness. The inset of Fig. 8 shows the T dependence of t^* for many film thicknesses for the rough substrate, and it appears that t^* grows less rapidly on cooling for increasingly thin films. Again, data for different substrate interactions show the same general trends.

We now use our data for t^* and τ to quantify the decoupling of relaxation time scales. Typically, this decoupling gives rise to a ‘fractional Stokes-Einstein’ (fSE) relation described by a power scaling law,

$$t^* \sim \tau^{1-\zeta}, \quad (7)$$

where $\zeta < 1$ is a fractional exponent characterizing the decoupling strength, so that $\zeta = 0$ defines the simple case where the Stokes-Einstein relation is valid. Figure 9 illustrates this variation for the representative case of polymer films on a rough substrate with $k = 100$ and $\varepsilon = 1.0$, where ζ ranges from roughly 0.65 in the thinnest film to 0.3 upon approaching the bulk limit. A similar increase of the decoupling strength ζ with increasing nanoparticle concentration has also been found in polymer nanocomposites for both attractive and non-attractive polymer-nanoparticle interactions [48].

The decoupling phenomenon is an inherently more complicated problem in polymeric materials than for small molecule liquids because there are separate relaxation timescales for the segmental motions within the chains and for center of mass motions (which occur at a much longer time scales associated with the displacement of the chain as whole). Recent work has shown that the fragility of the segmental and overall chain motion relaxation processes are generally quite different [49].

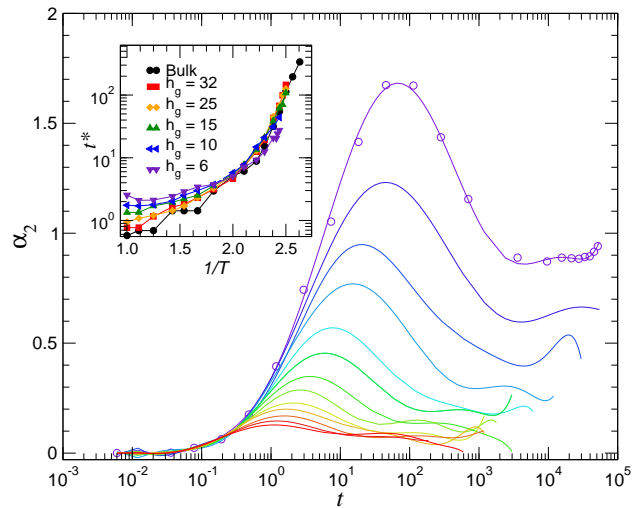


FIG. 8: The non-Gaussian parameter $\alpha_2(t)$ for various T for the case of film thickness 15 with a rough, attractive substrate ($\varepsilon = 1, k = 100$). The peak of $\alpha_2(t)$ defines the characteristic time scale t^* . The inset shows the T dependence of t^* for various film thicknesses. Data for other substrate interactions are qualitatively similar.

Moreover, Ediger and coworkers [50] found a complete absence of decoupling between the center of mass diffusion and shear viscosity in unentangled polystyrene over a wide temperature range. This situation is contrasted with relaxation at a segmental timescale where we observe a power law relation between τ and t^* . Sokolov and Schweitzer have separately considered a power law relation between the segmental τ and polymer chain relaxation time, which they also described as being a ‘decoupling’ relation [49]. We do not attempt to describe this result because the calculation of the chain relaxation time at low temperatures is computationally prohibitive, and because we do not believe that the ‘decoupling’ relationship of Sokolov and Schweitzer is analogous to the decoupling relation found in small molecule liquids. Of course, this relation between the segmental and large scale chain dynamics is fascinating and deserves further study.

We next consider experimental observations suggesting a direct relation between fragility and decoupling in small molecule glass formers. Decoupling in glass-forming liquids has mainly been studied in context of crystal growth [35, 51], where the decoupling exponent ζ is inferred indirectly from the relationship between the crystal growth cooling rate, and fluid viscosity. In particular Ref. [35], shows a proportional relation between m and ζ for low molecular weight organic and inorganic glass-forming liquids for a wide variation in fragility [35], although this work specifically excluded polymeric materials. Sokolov and Schweizer [49] studied the decoupling

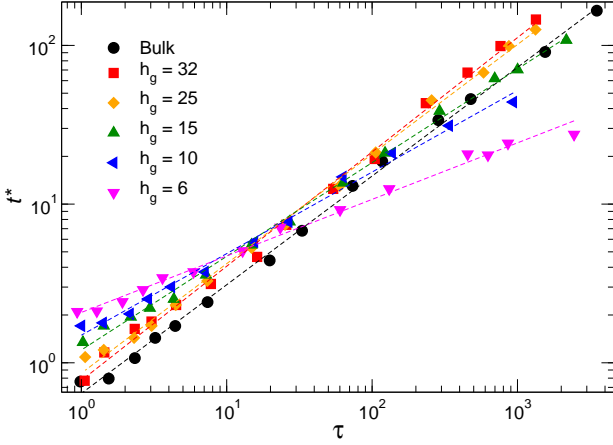


FIG. 9: Parametric relation between the coherent relaxation time τ and t^* for various film thickness for the representative case of a rough substrate with $k = 100$ and $\varepsilon = 1.0$, demonstrating a fractional power law relation $t^* \sim \tau^{1-\zeta}$. Clearly, ζ increases with decreasing film thickness as illustrated in Fig. 10.

exponent relating the segmental relaxation time and collective chain motion relaxation time for different polymer glass forming materials based on dielectric relaxation time measurements, and found a monotonic increase ζ with fragility for this type of decoupling. Together, these works suggest that the degree of decoupling might generally increase in systems having larger fragility, although there is no generally accepted theoretical understanding of why such a relation might exist.

We compared this trend to our results in Fig. 10, where we observe that the decoupling strength ζ increases with decreasing h_g for smooth and rough substrates. The inset of Fig. 10 illustrates how ζ varies with m , and we see that the relation between ζ and m does not follow a single trend in these two cases. A simple proportional relationship between ζ and m does not describe our data, raising a question about the general relation between decoupling strength and fragility. However, decoupling seems to be uniformly enhanced by geometrical confinement. Sengupta et al. [34] have observed a diminished decoupling in small molecule liquids between D and τ with an increase of spatial dimensionality. If we view making polymer films thinner as reducing the ‘effective’ spatial dimension, then our observations fully accord with those of Sengupta et al. Simulations of polymer nanocomposites also show a progressive reduction of fragility with nanoparticle concentration [38], an effect that might likewise be rationalized by an effective dimensional reduction with increased

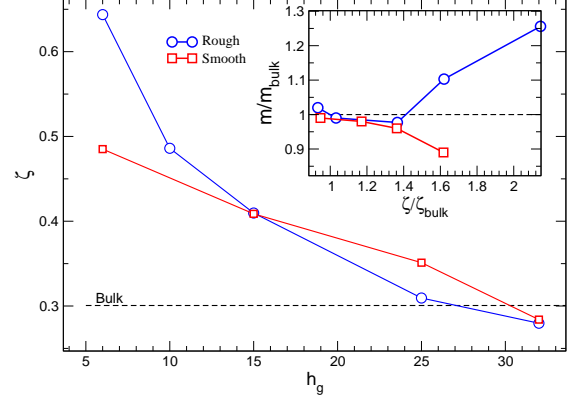


FIG. 10: Dependence of the decoupling exponent ζ on film thickness for rough and smooth substrate interactions when $k = 100$ and $\varepsilon = 1.0$. For both cases, ζ increases on decreasing thickness regardless of the type substrate interaction. The inset shows the relationship between relative ζ and relative m values obtained by altering the thickness of the film.

particle concentration, a point of view advocated previously [52]. While a definite relation between fragility and the strength of decoupling seems unlikely from the findings of Fig. 10, dimensionality does seem to be relevant to understanding this effect.

VI. COLLECTIVE MOTION IN THIN POLYMER FILMS

It has long been argued that polymer relaxation is governed by the scale of cooperative motion. From a theoretical perspective, the classical arguments of Adam-Gibbs (AG) [53], and our extension of this model based on numerical simulation evidence and thermodynamic modeling [54], provides a theoretical perspective for testing this proposition. Specifically, according to AG theory, the activation Gibbs free energy $\Delta G_a(T)$ is extensive of the size z^* of ‘cooperatively rearranging regions’ (CRR), so that τ can be formally written in terms of the general transition state theory relation,

$$\tau(T) = \tau_0 \exp[\Delta G_a(T)/k_B T], \quad \Delta G_a(T) \equiv z^* \Delta \mu \quad (8)$$

where $\Delta \mu$ is the activation free energy at high temperatures when particle motion does not involve a significant cooperative motion so that z^* equals a constant (AG originally assumed that $z^* \simeq 1$ at high temperatures, corresponding to completely uncooperative motion, but a constant value of z^* at high T is all that is required to recover Arrhenius dynamics). Recent simulations have shown that, despite the rather heuristic nature of the original arguments of AG, Eq. 8 with z^* identified specifically with the average size L of the cooperative

string-like particle exchange motion provides a good description for $\tau(T)$ in polymer melt simulations, even in the case when nanoparticles have been added to tune the fragility over a wide range [27, 36, 38, 55, 56]. Very recently, we have established a quantitative correspondence between the $L(T)$ and a living polymerization theory [54], and inspired by these results, Freed [57] has systematically derived Eq. 8 from transition state theory assuming that the transition states involve many-body transition events in the form of equilibrium polymers with z as the average string length. These results together provide a predictive theoretical framework for understanding the dynamics of glass-forming liquids.

We next evaluate $L(T)$ following methods described in previous works [36, 58, 59] to see if we can also describe the dynamics of thin polymer films within the same formalism. Figures 11 (a) and (b) compare the $L(T)$ for two film thicknesses with a rough or smooth substrate at two representative thicknesses. For a given film thickness, $L(T)$ is larger and grows faster for a film with rough substrate, which is qualitatively consistent with $\tau(T)$ (Fig. 1 (a) and (b)). The variation of $L(T)$ with substrate interaction strength ε or substrate rigidity k , shown in Figs. 11 (c) and (d), and $L(T)$ in these cases also qualitatively captures the variation of $\tau(T)$ (Figs. 5 (b) and (d)). The similarities between the variation of $L(T)$ and $\tau(T)$ suggest that we may be able to predict changes in fragility from the variation of $L(T)$, as found in previous works [18, 37, 38, 55]. Accordingly, in the following section we consider this possibility, and develop a framework to explain the variation of the activation parameters relating L and τ .

VII. COLLECTIVE MOTIONS AS AN ORGANIZING PRINCIPLE FOR THIN FILMS DYNAMICS

From the discussion of the preceding sections, it is clear that there are a variety of factors that can alter the dynamics of thin polymer films, including film thickness, roughness, the polymer-substrate interaction and the stiffness of the substrate. Impurities introduced from the film casting process and possible heterogeneity in the substrate chemistry due to, e.g., substrate oxidation, are also relevant [18]. These effects are all significant and the observed changes of the film dynamics involves the convolution of all these variables. We clearly need some organizing principle to explain how all these factors influence the film dynamics, and guide the development of polymer films with rationally engineered properties.

In this section, we explore a perspective that allows us to obtain a unified understanding of the diverse dynamical changes. The Adam-Gibbs perspective of the dynamics of glassy materials generally emphasizes the importance of collective molecular motion to understand rates of structural relaxation, and the results of the previous section indicate the promise of such an approach.

In order to quantitatively test Eq. 8, we follow Refs. [36–38, 60], and identify CRR size z^* with the relative size L/L_A of string-like cooperative particle arrangements. $L_A \equiv L(T_A)$ is the value of the string size at the temperature T_A , above which an Arrhenius law for $\tau(T)$ holds. To determine T_A , we use the same definition as in Ref. [54].

The analysis of the dynamics of our thin polymer films is then based on the string model for the dynamics of glass-forming liquids [54, 61], in which τ is described by the AG inspired relation,

$$\tau(h, T) = \tau_0(h) \exp \left[\frac{L(T)}{L_A(h)} \frac{\Delta\mu(h, T)}{k_B T} \right], \quad (9)$$

where $\Delta\mu(h, T)$ is the high temperature activation free energy for $T > T_A$,

$$\Delta\mu(h, T) = \Delta H_a(h) - T \Delta S_a(h), \quad (10)$$

where $\Delta H_a(h)$ and $\Delta S_a(h)$ are the enthalpic and the entropic contributions of the high T activation free energy respectively. These basic energetic parameters vary

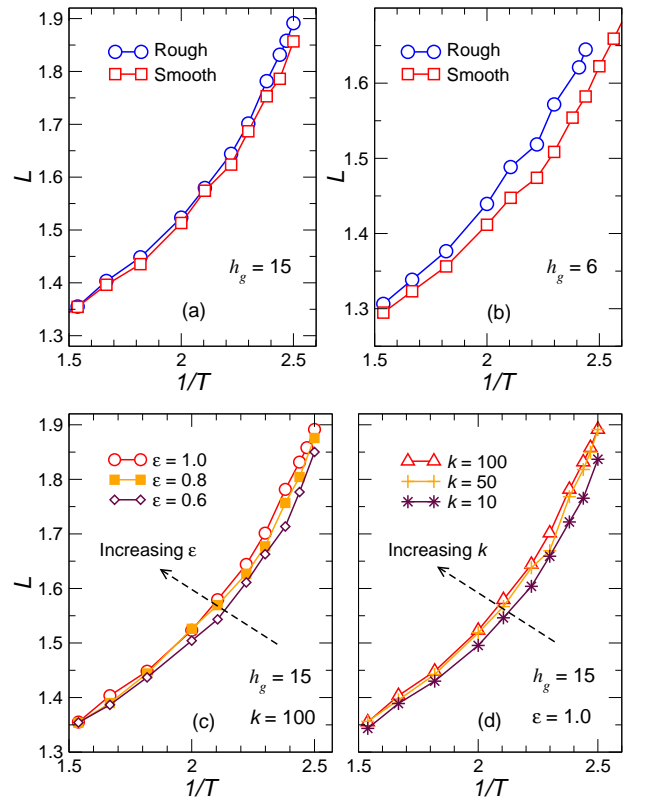


FIG. 11: Panels (a) and (b) show the comparison of $L(T)$ for films supported on a smooth or rough substrate. Panels (c) and (d) show the variation of $L(T)$ with varying polymer-substrate interaction ε or substrate rigidity k . The variation of $L(T)$ with h_g , ε and k mimics that of $\tau(T)$ shown in Figures 1 and 5. This qualitative consistency suggests the applicability of the string model of relaxation [54] to quantify $\tau(T)$.

with film thickness h_g and type of interaction (ε and k). Note that Eq. 9 for $T \geq T_A$ becomes, $\tau(h, T) = \tau_0 \exp[(\Delta\mu(h, T)/k_B T)]$, the typical activation form of transition state theory. In fact, Eq. 9 at T_A implies that $\tau_0(h)$ is not a free parameter, but instead is determined by

$$\tau_0(h) = \tau_A(h) \exp[-\Delta\mu(h, T_A(h))/k_B T_A(h)], \quad (11)$$

where $\tau_A \equiv \tau(T_A)$ so that ΔH_a and ΔS_a are the only undetermined parameters in Eq. 9. This relation was noted and tested in Ref. [61]. The string model prediction for the structural relaxation time of a film of thickness h can then be formally written,

$$\tau(h, T) = \tau_A(h) \exp \left[\frac{L(T)}{L_A(h)} \frac{\Delta\mu(h, T)}{k_B T} - \frac{\Delta\mu(h, T_A)}{k_B T_A} \right], \quad (12)$$

where, $\Delta H_a(h)$ and $\Delta S_a(h)$ are the only parameters on which τ depends, just as in ordinary transition state theory for homogeneous fluids.

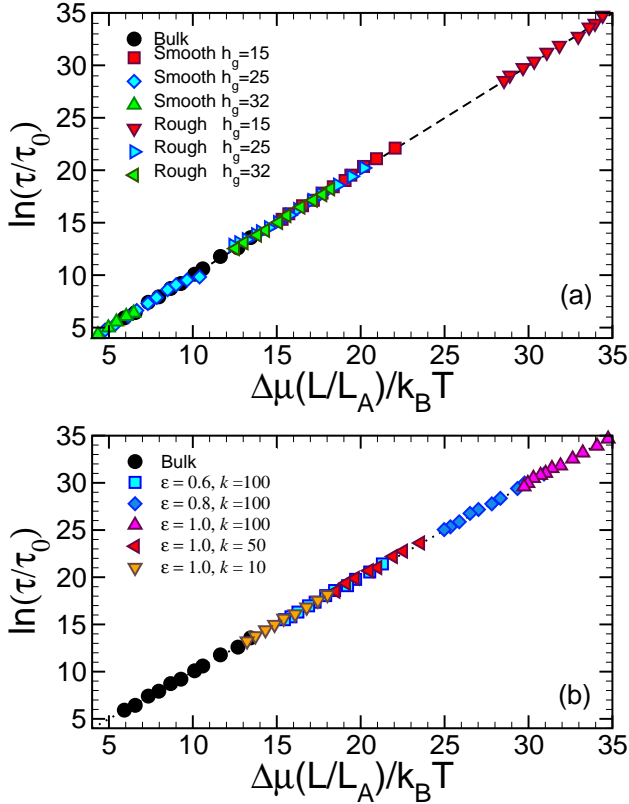


FIG. 12: Structural relaxation time τ in terms of the average strings size L for (a) various thicknesses, and (b) various polymer-substrate interactions or substrate rigidities. τ is scaled by $\tau_0 = \tau_A \exp[-\Delta\mu(T_A)/k_B T_A]$ where $\Delta\mu(T_A) = \Delta H_a - T_A \Delta S_a$, and ΔH_a and ΔS_a are determined by fitting to Eq. 9 over a broad T range.

We now demonstrate the applicability of Eq. 9 in quantitatively describing the dynamics of all the films we have

thus far studied. Figure 12 shows the linear relationship between $\ln(\tau)$ and $\Delta\mu L/k_B T$ for different films thickness in panel (a) and for different substrate rigidity and strength of interactions in panel (b). The universal collapse of τ in terms of string size was noted recently in a brief communications [55], but the variation of the relaxation time prefactor $\tau_0(h)$ was considered as a free parameter in that work. We find that this data reduction holds for all film thicknesses supported on a rough or smooth substrates, and applies as well as to the bulk polymer material. The same reduced variable description describes a representative film supported on a rough substrate for various substrate interaction or supporting substrate rigidity (see Fig. 12 (b)). Although the data reduction is identical between these figures, we separate them for clarity. This remarkable data reduction shows that we can quantitatively describe the film dynamics of all these films based on the string model relation (Eq. 9), despite a wide range of dynamical changes due to film thickness, polymer-substrate interaction, or substrate rigidity. For instance note that, Figs. 11(c) and (d) show that the average extent of cooperative motion L does not significantly change with ε or k , but that the structural relaxation time does change considerably. Therefore, the changes in τ must result from the variations of ΔH_a and ΔS_a , which we next discuss.

VIII. THEORY FOR THE CONFINEMENT EFFECTS ON ΔS_a AND ΔH_a

In order to develop a theoretical model of relaxation in polymer thin films (or polymers with molecular additives and nanocomposites), we must understand what controls the basic activation parameters ΔH_a and ΔS_a in the bulk polymer reference system. In general, the activation parameters at high T should depend on film thickness, since all these properties depend on the film thermodynamic properties. In this section, we specifically confront the issue of how the parameters ΔH_a and ΔS_a depend on film thickness, boundary geometry, and interaction strength. We begin by considering the variation of these energetic parameters in the high temperature limit, where cooperative motion does not complicate our discussion.

A. Transition State Theory

Classical transition state theory [62–64] implies that the diffusion coefficient, the structural relaxation time, and shear viscosity can all be described by an Arrhenius T dependence (at high T , where relaxation is not cooperative); i.e., the structural relaxation time τ can be expressed by the Arrhenius expression

$$\tau = \tau_0 \exp[\Delta G_a/k_B T], \quad (13)$$

where τ_0 is the vibrational time, and the activation free energy ΔG_a is associated with the displacement of a

polymer statistical segment [65, 66]. As discussed earlier, the activation free energy, $\Delta G_a(T > T_A) \equiv \Delta\mu$, has enthalpic contributions ΔH_a related to the strength of the intermolecular cohesive interactions, and entropic contributions ΔS_a arising from entropy changes needed to surmount complex multidimensional potential energy barriers in condensed materials [67–70]. Predicting ΔS_a is often a weak point in transition state modeling and the factor $\exp[-\Delta S_a/k_B]$ is often just absorbed into the measured prefactor τ_0 as a practical matter, but this is not an option for glass-forming liquids.

To guide our thinking, we need to recognize the physical origin for the values of ΔH_a and ΔS_a . In order to understand qualitatively ΔH_a , we go back to Eyring’s early transition state theory arguments [64], and consider long-standing physical observations in simple fluids [71–73] that relate ΔH_a to the energy change associated with the removal of a test molecule from its local environment in the fluid state [74–76]. Such, an interpretation has recently been implemented computationally by Egami and coworkers [77]. This perspective implies that ΔH_a should scale in approximate proportion to the heat of vaporization H_{vap} or the cohesive interaction energy of the fluid. Although this argument is simple, its experimental validity has been established for hundreds of fluids [78]. More recently, simulations of simple Lennard-Jones fluids in 2 and 3 dimensions have shown that ΔH_a scales in proportion to the interaction parameter ε [79–81], the natural measure of intermolecular interaction strength in simple pair potential models such as LJ fluids and also our polymer model.

As noted above, the variation of ΔS_a with molecular parameters is less well understood. In many small molecule fluids, the intermolecular potential is weak, and therefore the variation of ΔS_a can be reasonably neglected. However, for molecules with many internal degrees of freedom, such as polymers, there can be a considerable variation in ΔS_a . In particular, a survey by Bondi [67] revealed that $\Delta S_a/k_B$ could vary over a 100 units, and can even change sign, so that variations of ΔS_a cannot be ignored. Bondi’s pioneering study describes the frustrations of early theoretical efforts to estimate ΔS_a theoretically for complex fluids.

The basic physical picture that the free energy of activation is related to the free energy cost of removing a molecule from its local molecular environment suggests a proportionate contribution to ΔS_a from the cohesive intermolecular interaction [70, 82]. This effect is evident in Trouton’s rule [83, 84], which relates the heat of vaporization H_{vap} and the entropy of vaporization S_{vap} of gases and the Barclay-Butler phenomenological relation linking enthalpies and entropies of solvation in many mixtures [85–88]. Indeed, many studies have established the specific relation [68–70],

$$\Delta S_a = \Delta S_0 + \Delta H_a/k_B T_{\text{comp}} \quad (14)$$

supported by observations on diverse materials, where ΔS_0 captures a background contribution associated with

the internal configurational degrees of freedom of fluid molecules. This linear relation has long been established for the Arrhenius activation parameters of bulk polymer fluids [89, 90]. In glass-forming materials, the entropy-enthalpy ‘compensation temperature’ T_{comp} is often found to be near the glass transition temperature of the fluid sometimes termed, the “melting temperature of the glass” [91]; in crystalline solid materials, T_{comp} is often found to be near the melting temperature T_m of the solid [92, 93]. We indeed find ‘entropy-enthalpy’ compensation in our simulated glass-forming films (shown in Fig. 13) where the compensation temperature, $T_{\text{comp}} = 0.18$, a temperature similar to the estimated VFT temperature. These observations suggest that T_{comp} is determined by a physical condition at which the intermolecular cohesive interaction is insufficient to keep the material in the solid state, so that the fluid then begins to explore liquid-like configurations, but a quantitative understanding of how T_{comp} relates to the structure of the potential energy substrate remains to be determined. We next examine how ΔH_a and ΔS_a of transition state theory depend on the scale of confinement in thin polymer films.

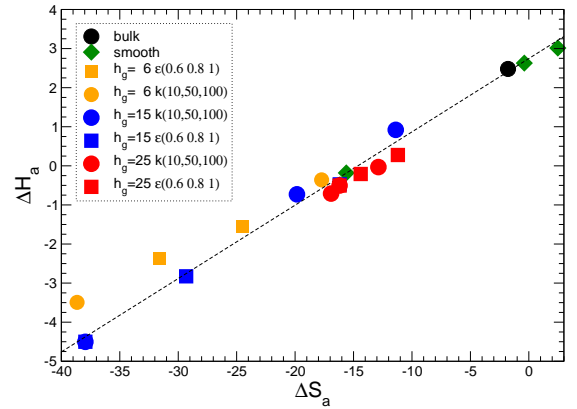


FIG. 13: Variation of ΔH_a and ΔS_a for different film thicknesses, substrate roughnesses, substrate interactions, and substrate rigidities. The slope defines compensation temperature $T_{\text{comp}} = 0.18$. The data for the thinnest film ($h_g = 6$) shows a deviation from the thicker film data, which is discussed in the main text.

B. Effect of confinement on ΔH_a and ΔS_a

In general, film confinement (or the addition of additives to a fluid) must change the effective molecular coordination number, and thus the cohesive interaction strength, so that $\Delta S_a(h)$ and $\Delta H_a(h)$ of activation also vary with film thickness and boundary interactions. This change in the effective coordination number due to

changes in the surface-to-volume ratio with confinement has been extensively discussed in connection to estimate critical point shifts in confined fluids and magnetic materials [94, 95], and as the origin of the Gibbs-Thomson effect for the shift of the melting point of crystals [96]. This scaling argument suggests that $\Delta H_a(h)$ scales with the substrate-to-volume ratio of the film, so that

$$\Delta H_a(h) - \Delta H_a(\text{bulk}) \sim 1/h. \quad (15)$$

We see that this scaling is roughly consistent with the data in Fig. 14, but varying the substrate energy of the film can also lead to a change in ΔH_a , whose sign depends on whether substrate-polymer interactions are stronger or weaker than the polymer-fluid interactions. In particular, Fig. 14 shows that ΔH_a decreases with k and ε . Thus, there are a number of contributing substrate terms that influence ΔH_a so a clean $\sim 1/h$ finite size scaling of ΔH_a is not obtained. Nonetheless, the general trend in variation of ΔH_a with confinement is understandable. We emphasize that despite the highly variable nature of the variation of ΔH_a and ΔS_a with boundary interaction, roughness, substrate rigidity and film thickness, the compensation relation between these activation energies holds to an excellent approximation. However, there is a different relation between ΔH_a and ΔS_a for film thickness $h_g = 6$, an effect that is also reflected of the increase in the decoupling exponent ζ in Fig. 9. This interesting effect requires further study, but it may be a consequence of the strong deviation of ρ from its bulk value very near the substrate. In particular, Fig. 7 shows large density gradients for $z < 6$, so that ‘ultrathin’ films with $h_g \lesssim 6$ are rather unlike the bulk material and thicker polymer films. The component of ΔS_a that is linked to ΔH_a is expected from entropy-enthalpy compensation to follow the same dependence as ΔH_a , suggesting a similar inverse dependence on thickness. Fig. 15(c) shows this is the case.

We have not previously discussed the relaxation time prefactor τ_0 in Eq. 9, which varies appreciably with confinement, as shown in Fig. 16 for thin polymer films on smooth or rough substrates. In particular, Fig. 16 indicates that the changes in τ_0 can be as large as *10 orders of magnitude*, so this factor is highly relevant for understanding the changes in relaxation time in thin films and nanocomposites. We again emphasize that τ_0 is not a free parameter in the string model of glass-formation, but this quantity is entirely determined from ΔH_a and ΔS_a (Eq. 11).

Although τ_0 varies strongly with confinement, the relaxation time at T_A , τ_A varies only weakly, so that τ_0 changes are due almost entirely to changes of $\Delta H_a(h)$ and $\Delta S_a(h)$. This phenomenon has not been appreciated before. Evidently, the significant changes in the relaxation of glass-forming films and nanocomposites derive in large part from the high temperature activation parameters, which are typically thought not to have a direct relation to glass formation.

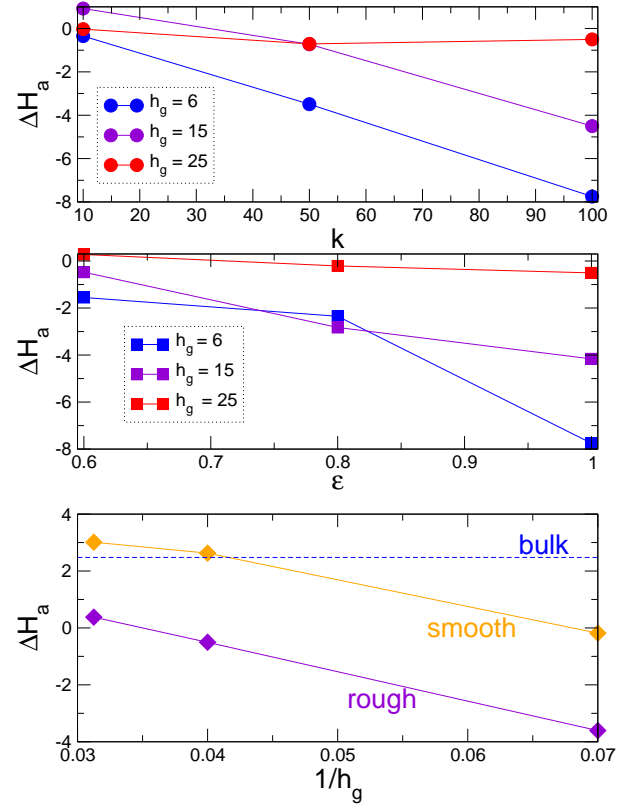


FIG. 14: Changes in the enthalpic contribution ΔH_a of the activation free energy. (a) Effect of varying the roughness by varying k_s . (b) Effect of varying the strength of the substrate interaction by varying ε . (c) Changing confinement on smooth or rough films.

IX. CONCLUSIONS

We have systematically explored factors that alter the dynamics of thin supported polymer films—film thickness, substrate roughness, polymer-substrate interaction strength, and the rigidity of the supporting substrate. All these factors were found to be highly relevant to the dynamics of our simulated polymer films and their coupling makes an understanding of changes in polymer film dynamics in thin films rather complicated. Simple free volume ideas are inadequate to explain the significant changes that we observe. Control of boundary roughness and polymer-substrate interaction is evidently necessary to make polymer films with reproducible properties and the prediction of film properties based on computation will require the specification of many factors related to the film boundary conditions and structure.

Despite the wide variation of film dynamics with boundary conditions and film thickness, we find that we can obtain a remarkably general characterization of the changes in the film dynamics for all film conditions using the string model of structural relaxation. In particular, we quantitatively describe the change in dynamics of sup-

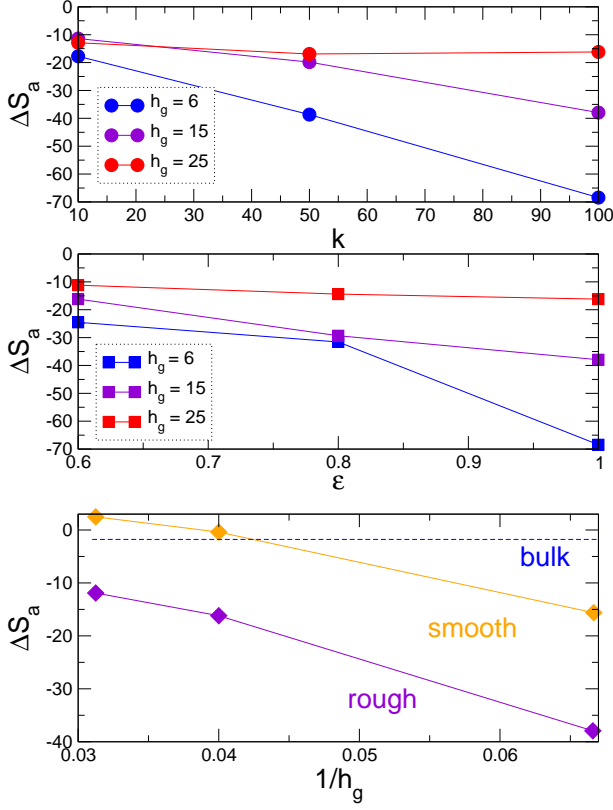


FIG. 15: Changes in the entropic contribution ΔS_a of the activation free energy. (a) Effect of varying the roughness by varying the parameter k_s . (b) Effect of varying the strength of the substrate interaction by varying the parameter ϵ . (c) Changing confinement on smooth or rough films.

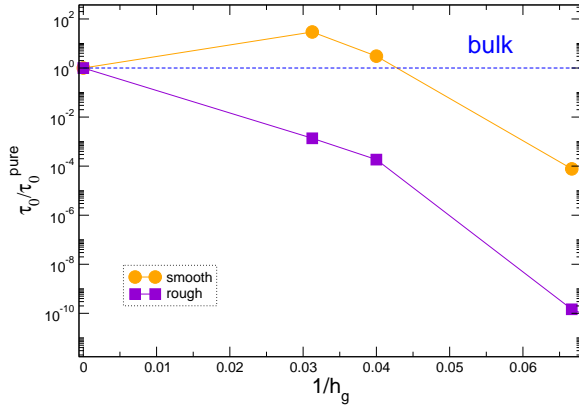


FIG. 16: Changes in τ_0 as a function of inverse of film thickness relative to the value for the bulk system, as a function of the inverse of the thickness h_g . The circles represent smooth substrate and the squares represent those for a rough substrate.

ported polymer films based on how the collective motion is perturbed in the film. These changes are ultimately parameterized in terms of the high temperature activation free energy, leading to the almost paradoxical finding that glass formation is controlled by the fluid properties in the high temperature limit.

Given the computational success of the string model, we are now faced with the problem of determining the extent of string-like collective motion in real materials. Future work must address how the extent of collective motion can be effectively estimated from direct measurement. Our recent measurements [54] suggest a direct relation between the string length and the interfacial mobility scale near the polymer-air boundary of supported films and offers a promising method for estimating the string length. Moreover, recent work [97] also suggests that noise measurements might be effective for estimating average string length, and we plan to pursue this possibility in the future.

As a secondary consideration, we examined how the large changes in fragility in our simulations were related to changes between a diffusive relaxation time and the decoupling relation in the segmental relaxation time. We find that decoupling and fragility can change in opposing directions, calling into question a general relation between decoupling and fragility. However, the changes in the decoupling exponent ζ are in accord with simulation results [34] and theoretical arguments [52] for the effect of reduced dimensionality on decoupling. Thus, our findings do not support previous observations indicating a proportional change between fragility and the strength of decoupling in small molecule liquids, and we conclude that the relation between fragility and decoupling requires further study. Our observations also imply that it would be worthwhile to define the concept of effective dimensionality more precisely and check this perspective with changes of the decoupling strength.

- [1] D. Bratton, D. Yang, J. Y. Dai, and C. K. Ober, *Polym. Adv. Tech.* **17**, 94 (2006).
- [2] D. W. Huttmacher, *J. Biomat. Sci. Polym. Ed.* **12**, 107 (2001), ISSN 0920-5063.
- [3] C. M. Stafford, B. D. Vogt, C. Harrison, D. Julthongpiput, and R. Huang, *Macromolecules* **39**, 5095 (2006), URL <http://dx.doi.org/10.1021/ma060790i>.
- [4] P. A. O'Connell, S. A. Hutcheson, and G. B. McKenna, *J. Polym. Sci. B* **46**, 1952 (2008), URL <http://dx.doi.org/10.1002/polb.21531>.
- [5] M. Alcoutlabi and G. B. McKenna, *J. Phys. Condens. Matter* **17**, R461 (2005), ISSN 0953-8984.
- [6] K. Binder, J. Horbach, R. Vink, and A. De Virgiliis, *Soft Matter* **4**, 1555 (2008), ISSN 1744-683X.
- [7] J. L. Keddie, R. A. L. Jones, and R. A. Cory, *Europhys. Lett.* **27**, 59 (1994).
- [8] J. A. Forrest, K. Dalnoki-Veress, and J. R. Dutcher, *Phys. Rev. E* **56**, 5705 (1997), ISSN 1063-651X.
- [9] K. Fukao and Y. Miyamoto, *Phys. Rev. E* **64**, 011803 (2001), URL <http://link.aps.org/doi/10.1103/PhysRevE.64.011803>.
- [10] D. S. Fryer, R. D. Peters, E. J. Kim, J. E. Tomaszewski, J. J. de Pablo, P. F. Nealey, C. C. White, and W. L. Wu, *Macromolecules* **34**, 5627 (2001), ISSN 0024-9297.
- [11] C. J. Ellison and J. M. Torkelson, *Nature Materials* **2**, 695 (2003), ISSN 1476-1122.
- [12] A. Bansal, H. C. Yang, C. Z. Li, K. W. Cho, B. C. Benicewicz, S. K. Kumar, and L. S. Schadler, *Nature Materials* **4**, 693 (2005), ISSN 1476-1122.
- [13] R. D. Priestley, C. J. Ellison, L. J. Broadbelt, and J. M. Torkelson, *Science* **309**, 456 (2005), ISSN 0036-8075.
- [14] S. Kim, S. A. Hewlett, C. B. Roth, and J. M. Torkelson, *Eur. Phys. J. E* **30**, 83 (2009), ISSN 1292-8941.
- [15] J. A. Torres, P. F. Nealey, and J. J. de Pablo, *Phys. Rev. Lett.* **85**, 3221 (2000), ISSN 0031-9007.
- [16] G. D. Smith, D. Bedrov, and O. Borodin, *Phys. Rev. Lett.* **90**, 226103 (2003), URL <http://link.aps.org/doi/10.1103/PhysRevLett.90.226103>.
- [17] J. Baschnagel and F. Varnick, *Condensed Matter* **17**, 852 (2005).
- [18] R. A. Riggelman, K. Yoshimoto, J. F. Douglas, and J. J. de Pablo, *Phys. Rev. Lett.* **97**, 045502 (2006), ISSN 0031-9007.
- [19] S. Peter, H. Meyer, and J. Baschnagel, *J. Chem. Phys.* **131**, 014902 (2009), ISSN 0021-9606.
- [20] J.-L. Barrat, J. Baschnagel, and A. Lyulin, *Soft Matter* **6**, 3430 (2010).
- [21] J. A. Forrest, K. Dalnoki-Veress, J. R. Stevens, and J. R. Dutcher, *Phys. Rev. Lett.* **77**, 2002 (1996), ISSN 0031-9007.
- [22] K. Paeng, R. Richert, and M. D. Ediger, *Soft Matter* **8**, 819 (2012), URL <http://dx.doi.org/10.1039/C1SM06501G>.
- [23] C. J. Ellison, S. D. Kim, D. B. Hall, and J. M. Torkelson, *Eur. Phys. J. E* **8**, 155 (2002), ISSN 1292-8941.
- [24] A. Schönhals, H. Goering, C. Schick, B. Frick, and R. Zorn, *Eur. Phys. J. E* **12**, 173 (2003), ISSN 1292-8941.
- [25] S. Kawana and R. A. L. Jones, *Phys. Rev. E* **63**, 021501 (2001), ISSN 1063-651X.
- [26] S. Peter, H. Meyer, and J. Baschnagel, *J. Polym. Sci. B* **44**, 2951 (2006), ISSN 0887-6266.
- [27] P. Z. Hanakata, J. F. Douglas, and F. W. Starr, *The Journal of Chemical Physics* **137**, 244901 (2012), URL <http://scitation.aip.org/content/aip/journal/jcp/137/24/10.1063/1.4772402>.
- [28] C. B. Roth, K. L. McNerny, W. F. Jager, and J. M. Torkelson, *Macromolecules* **40**, 2568 (2007), <http://pubs.acs.org/doi/pdf/10.1021/ma062864w>, URL <http://pubs.acs.org/doi/abs/10.1021/ma062864w>.
- [29] R. S. Tate, D. S. Fryer, S. Pasqualini, M. F. Montague, J. J. de Pablo, and P. F. Nealey, *J. Chem. Phys.* **115**, 9982 (2001), URL <http://scitation.aip.org/content/aip/journal/jcp/115/21/10.1063/1.1415497>.
- [30] M. Erber, M. Tress, E. U. Mapesa, A. Serghei, K.-J. Eichhorn, B. Voit, and F. Kremer, *Macromolecules* **43**, 7729 (2010), <http://pubs.acs.org/doi/pdf/10.1021/ma100912r>, URL <http://pubs.acs.org/doi/abs/10.1021/ma100912r>.
- [31] Q. Tong and S. J. Sibener, *Macromolecules* **46**, 8538 (2013), <http://pubs.acs.org/doi/pdf/10.1021/ma401629s>, URL <http://pubs.acs.org/doi/abs/10.1021/ma401629s>.
- [32] D. Hudzinsky, A. V. Lyulin, A. R. C. Baljon, N. K. Balabaev, and M. A. J. Michels, *Macromolecules* **44**, 2299 (2011), <http://pubs.acs.org/doi/pdf/10.1021/ma102567s>, URL <http://pubs.acs.org/doi/abs/10.1021/ma102567s>.
- [33] C. Batistakis, A. V. Lyulin, and M. A. J. Michels, *Macromolecules* **45**, 7282 (2012), <http://pubs.acs.org/doi/pdf/10.1021/ma300753e>, URL <http://pubs.acs.org/doi/abs/10.1021/ma300753e>.
- [34] S. Sengupta, S. Karmakar, C. Dasgupta, and S. Sastry, *J. Chem. Phys.* **138**, 12A548 (2013).
- [35] M. D. Ediger, P. Harrowell, and L. Yu, *J. Chem. Phys.* **128**, 034709 (2008), URL <http://scitation.aip.org/content/aip/journal/jcp/128/3/10.1063/1.2815325>.
- [36] F. W. Starr, J. F. Douglas, and S. Sastry, *J. Chem. Phys.* **138**, 12A541 (2013).
- [37] F. W. Starr and J. F. Douglas, *Phys. Rev. Lett.* **106**, 115702 (2011).
- [38] B. A. Pazmino Betancourt, J. F. Douglas, and F. W. Starr, *Soft Matter* **9**, 241 (2013), URL <http://dx.doi.org/10.1039/C2SM26800K>.
- [39] P. Scheidler, W. Kob, and K. Binder, *Europhys. Lett.* **59**, 701 (2002), URL <http://stacks.iop.org/0295-5075/59/i=5/a=701>.
- [40] A. Virgiliis, A. Milchev, V. Rostiasvili, and T. Vilgis, *Eur. Phys. J. E* **35**, 1 (2012), ISSN 1292-8941, URL <http://dx.doi.org/10.1140/epje/i2012-12097-6>.
- [41] C. Angell, *Polymer* **38**, 6261 (1997), ISSN 0032-3861, URL <http://www.sciencedirect.com/science/article/pii/S0032386197002012>.
- [42] C. A. Angell, *Science* **267**, 1924 (1995).
- [43] Q. Qin and G. B. McKenna, *J. Non-Cryst. Solids* **352**, 2977 (2006), ISSN 0022-3093.
- [44] K. Binder, J. Baschnagel, and W. Paul, *Prog. Polym. Sci.* **28**, 115 (2003), ISSN 0079-6700.
- [45] H. Yamakawa, *Modern Theory of Polymer Solutions* (Harper and Row Publishers, 1971).
- [46] K. F. Freed, *Journal of Physics A: Mathematical and General* **18**, 871 (1985), URL <http://stacks.iop.org/>

- 0305-4470/18/i=5/a=019.
- [47] J. F. Douglas, *Macromolecules* **22**, 3707 (1989), <http://dx.doi.org/10.1021/ma00199a035>, URL <http://dx.doi.org/10.1021/ma00199a035>.
 - [48] B. A. Pazmiño Betancourt, F. W. Starr, and J. F. Douglas (2014), in preparation.
 - [49] A. P. Sokolov and K. S. Schweizer, *Phys. Rev. Lett.* **102**, 248301 (2009), URL <http://link.aps.org/doi/10.1103/PhysRevLett.102.248301>.
 - [50] O. Urakawa, S. F. Swallen, M. D. Ediger, and E. D. von Meerwall, *Macromolecules* **37**, 1558 (2004), <http://dx.doi.org/10.1021/ma0352025>, URL <http://dx.doi.org/10.1021/ma0352025>.
 - [51] M. K. Mapes, S. F. Swallen, and M. D. Ediger, *The Journal of Physical Chemistry B* **110**, 507 (2006), pMID: 16471562, <http://dx.doi.org/10.1021/jp0555955>, URL <http://dx.doi.org/10.1021/jp0555955>.
 - [52] J. F. Douglas and T. Ishinabe, *Phys. Rev. E* **51**, 1791 (1995), URL <http://link.aps.org/doi/10.1103/PhysRevE.51.1791>.
 - [53] G. Adam and J. H. Gibbs, *J. Chem. Phys.* **43**, 139 (1965), ISSN 0021-9606.
 - [54] B. A. Pazmiño Betancourt, J. F. Douglas, and F. W. Starr, *The Journal of Chemical Physics* **140**, 204509 (2014), URL <http://scitation.aip.org/content/aip/journal/jcp/140/20/10.1063/1.4878502>.
 - [55] P. Z. Hanakata, J. F. Douglas, and F. W. Starr, *Nature Communications* **5**, 256207 (2014).
 - [56] In their original work, AG identified z^* with the minimal scale of cooperative movement while we identify z with the average over a highly polydisperse distribution of collective movements observed in our simulations. This is an important conceptual difference between the string model and the AG model, but both models lead to Eq. 8 as their final result so that the string model is certainly preserves the spirit of the AG relation.
 - [57] K. F. Freed, *The Journal of Chemical Physics* **141**, 141102 (2014), URL <http://scitation.aip.org/content/aip/journal/jcp/141/14/10.1063/1.4897973>.
 - [58] C. Donati, J. F. Douglas, W. Kob, S. J. Plimpton, P. H. Poole, and S. C. Glotzer, *Phys. Rev. Lett.* **80**, 2338 (1998), URL <http://link.aps.org/doi/10.1103/PhysRevLett.80.2338>.
 - [59] M. Aichele, Y. Gebremichael, F. Starr, J. Baschnagel, and S. Glotzer, *J. Chem. Phys.* **119**, 5290 (2003).
 - [60] F. W. Starr, P. Z. Hanakata, B. A. P. Betancourt, S. Sastri, and J. F. Douglas, *Fragility and Cooperative Motion in Polymer Glass Formation* (Fragility of glass forming liquids, 2014).
 - [61] B. A. Pazmiño Betancourt, P. Z. Hanakata, F. W. Starr, and J. F. Douglas (2014), submitted.
 - [62] H. Eyring, *J. Chem. Phys.* **4**, 283 (1936), URL <http://scitation.aip.org/content/aip/journal/jcp/4/4/10.1063/1.1749836>.
 - [63] R. H. Ewell, *J. Appl. Phys.* **9**, 252 (1938), URL <http://scitation.aip.org/content/aip/journal/jap/9/4/10.1063/1.1710415>.
 - [64] S. Glasstone, K. J. Laidler, and H. Eyring, *Theory of Rate Processes* (McGraw Hill, 1941), first edition ed., URL <http://www.amazon.com/exec/obidos/redirect?tag=citeulike07-20&path=ASIN/B000IXRJ6W>.
 - [65] W. Kauzmann and H. Eyring, *J. Am. Chem. Soc.* **62**, 3113 (1940), <http://pubs.acs.org/doi/pdf/10.1021/ja01868a059>, URL <http://pubs.acs.org/doi/abs/10.1021/ja01868a059>.
 - [66] H. Eyring, T. Ree, and N. Hirai, *Proc. Natl. Acad. Sci. USA* **44**, 1213 (1958), <http://www.pnas.org/content/44/12/1213.full.pdf+html>, URL <http://www.pnas.org/content/44/12/1213.short>.
 - [67] A. Bondi, *J. Chem. Phys.* **14**, 591 (1946), URL <http://scitation.aip.org/content/aip/journal/jcp/14/10/10.1063/1.1724071>.
 - [68] A. Yelon, B. Movaghar, and R. S. Crandall, *Rep. Prog. Phys.* **69**, 1145 (2006), URL <http://stacks.iop.org/0034-4885/69/i=4/a=R04>.
 - [69] A. Yelon, E. Sacher, and W. Linert, *Catalysis Letters* **141**, 954 (2011), ISSN 1011-372X, URL <http://dx.doi.org/10.1007/s10562-011-0645-8>.
 - [70] A. Yelon and B. Movaghar, *Phys. Rev. Lett.* **65**, 618 (1990), URL <http://link.aps.org/doi/10.1103/PhysRevLett.65.618>.
 - [71] E. W. Madge, *J. Appl. Phys.* **5**, 39 (1934), URL <http://scitation.aip.org/content/aip/journal/jap/5/2/10.1063/1.1745228>.
 - [72] F. Eirich and R. Simha, *J. Chem. Phys.* **7**, 116 (1939), URL <http://scitation.aip.org/content/aip/journal/jcp/7/2/10.1063/1.1750389>.
 - [73] L. Qun-Fang, H. Yu-Chun, and L. Rui-Sen, *Fluid Phase Equilibria* **140**, 221 (1997), ISSN 0378-3812, URL <http://www.sciencedirect.com/science/article/pii/S0378381297001763>.
 - [74] E. W. Madge, *Journal of Applied Physics* **5**, 39 (1934), URL <http://scitation.aip.org/content/aip/journal/jap/5/2/10.1063/1.1745228>.
 - [75] F. Eirich and R. Simha, *The Journal of Chemical Physics* **7**, 116 (1939), URL <http://scitation.aip.org/content/aip/journal/jcp/7/2/10.1063/1.1750389>.
 - [76] S. Glasstone, K. Laidler, and H. Eyring, *The Theory of Rate Processes: The Kinetics of Chemical Reactions, Viscosity, Diffusion and Electrochemical Phenomena*, International chemical series (McGraw-Hill Book Company, Incorporated, 1941), URL <http://books.google.com/books?id=zb2GAAAAIAAJ>.
 - [77] T. Iwashita, D. M. Nicholson, and T. Egami, *Phys. Rev. Lett.* **110**, 205504 (2013), URL <http://link.aps.org/doi/10.1103/PhysRevLett.110.205504>.
 - [78] L. Qun-Fang, H. Yu-Chun, and L. Rui-Sen, *Fluid Phase Equilibria* **140**, 221 (1997), ISSN 0378-3812, URL <http://www.sciencedirect.com/science/article/pii/S0378381297001763>.
 - [79] R. Speedy, F. Prielmeier, T. Vardag, E. Lang, and H.-D. Lüdemann, *Mol. Phys.* **66**, 577 (1989), URL <http://www.tandfonline.com/doi/abs/10.1080/00268978900100341>.
 - [80] H. G. E. Hentschel, S. Karmakar, I. Procaccia, and J. Zylberg, *ArXiv e-prints* (2012), 1202.1127.
 - [81] T. Iwashita, D. M. Nicholson, and T. Egami, *Phys. Rev. Lett.* **110**, 205504 (2013), URL <http://link.aps.org/doi/10.1103/PhysRevLett.110.205504>.
 - [82] G. Boisvert, N. Mousseau, and L. J. Lewis, *Phys. Rev. Lett.* **80**, 203 (1998), URL <http://link.aps.org/doi/10.1103/PhysRevLett.80.203>.
 - [83] R. M. Digilov and M. Reiner, *Eur. J. Phys.* **25**, 15 (2004), URL <http://stacks.iop.org/0143-0807/25/i=1/a=003>.
 - [84] L. K. Nash, *J. Chem. Ed.* **61**, 981 (1984),

- <http://pubs.acs.org/doi/pdf/10.1021/ed061p981>, URL <http://pubs.acs.org/doi/abs/10.1021/ed061p981>.
- [85] I. M. Barclay and J. A. V. Butler, *Trans. Faraday Soc.* **34**, 1445 (1938), URL <http://dx.doi.org/10.1039/TF9383401445>.
- [86] R. P. Bell, *Trans. Faraday Soc.* **33**, 496 (1937), URL <http://dx.doi.org/10.1039/TF9373300496>.
- [87] M. G. Evans and M. Polanyi, *Trans. Faraday Soc.* **32**, 1333 (1936), URL <http://dx.doi.org/10.1039/TF9363201333>.
- [88] H. S. Frank, *J. Chem. Phys.* **13**, 493 (1945), URL <http://scitation.aip.org/content/aip/journal/jcp/13/11/10.1063/1.1723984>.
- [89] R. M. Barrer, *Trans. Faraday Soc.* **39**, 48 (1943), URL <http://dx.doi.org/10.1039/TF9433900048>.
- [90] C. E. Waring and P. Becher, *J. Chem. Phys.* **15**, 488 (1947), URL <http://scitation.aip.org/content/aip/journal/jcp/15/7/10.1063/1.1746569>.
- [91] J. C. Dyre, *J. Phys. C* **19**, 5655 (1986), URL <http://stacks.iop.org/0022-3719/19/i=28/a=016>.
- [92] R. K. Eby, *The Journal of Chemical Physics* **37**, 2785 (1962), URL <http://scitation.aip.org/content/aip/journal/jcp/37/12/10.1063/1.1733106>.
- [93] G. J. Dienes, *Journal of Applied Physics* **21**, 1189 (1950), URL <http://scitation.aip.org/content/aip/journal/jap/21/11/10.1063/1.1699563>.
- [94] M. E. Fisher and A. E. Ferdinand, *Phys. Rev. Lett.* **19**, 169 (1967), URL <http://link.aps.org/doi/10.1103/PhysRevLett.19.169>.
- [95] G. A. T. Allan, *Phys. Rev. B* **1**, 352 (1970), URL <http://link.aps.org/doi/10.1103/PhysRevB.1.352>.
- [96] C. L. Jackson and G. B. McKenna, *The Journal of Chemical Physics* **93**, 9002 (1990), URL <http://scitation.aip.org/content/aip/journal/jcp/93/12/10.1063/1.459240>.
- [97] H. Zhang and J. F. Douglas, *Soft Matter* **9**, 1254 (2013), URL <http://dx.doi.org/10.1039/C2SM26789F>.